

Effect of ZnO films on CdTe solar cells*

Liu Tingliang(刘庭良), He Xulin(何绪林), Zhang Jingquan(张静全)[†], Feng Lianghuan(冯良桓), Wu Lili(武莉莉), Li Wei(李卫), Zeng Guanggen(曾广根), and Li Bing(黎兵)

College of Materials Science & Engineering, Sichuan University, Chengdu 610064, China

Abstract: The ZnO high resistivity transparent (HRT) layers were prepared by DC magnetron sputtering on the 1 mm borosilicate glass with 150 nm ITO coating. The structural, optical and electrical properties of the as-deposited films were investigated by XRD, UV/Vis spectroscopy and four-probe technology. The interface characters of the ITO/ZnO and ZnO/CdS systems were studied by ultraviolet photoelectron spectroscopy (UPS) and X-ray photoelectron spectroscopy (XPS) depth profiling tests. The results show that ZnO has good optical and electrical properties. The insertion of the ZnO films decreases the energy barrier between ITO and CdS films. The energy conversion efficiency and quantum efficiency were found to be 12.77% (8.9%) and > 90% (79%) with or (without) ZnO films of CdTe solar cells. Furthermore, the effect of thickness, mobility and carrier density of ZnO films on CdTe solar cells was analyzed by AMPD-1D.

Key words: ZnO; HRT; CdTe solar cells; XPS; UPS

DOI: 10.1088/1674-4926/33/9/093003

PACC: 7360L; 7340

1. Introduction

Thin film CdTe/CdS solar cells are typically of the configuration. One of the important CdTe technology issues is the fabrication of thin CdS films. Thin CdS films can lead to increase the number of incident photons that reach the CdTe and therefore increase the efficiency. Wu^[1] and Romeo^[2] have reported the efficiency of 16.5% and 15.8% with < 100 nm and 80 nm CdS thickness, respectively. However, as the thickness of CdS is decreased, the films would become discontinuous leading to the formation of localized CdTe/TCO junction, which lead to excessive shunting and therefore lower the solar cell efficiency^[3]. The deposition of pinhole free CdS films is critical in achieving high solar cell efficiencies. Using high resistivity transparent (HRT) layers are known as a feasible method to improve the characteristics of CdTe thin films solar cells. The uses of HRT layers between TCO and CdS layers have been reported to improve the CdS film morphology by providing large grains during deposition^[4] and increase the device performance, such as the short-circuit current density (I_{sc}), the open voltage (V_{oc}), or the filling factor (FF)^[5].

The HRT layers in CdTe solar cells include SnO₂, Al₂O₃, ZnSnO₄ et al. Andreas Klein^[6] and Hasitha Mahabaduge^[7] have summarized and compared the characterization of ZnO, SnO₂ and Al₂O₃ layers as high resistance transparent conducting oxides. S N Alamri and A W Brinkman^[8] have fabricated and studied the efficiency of CdTe solar cells with SnO_x as HRT layers. A. Fuchs et al.^[9] have studied SnO₂ layers as HRT in CdTe solar cells by XPS. The ZnO has the direct energy gap structure of 3.37eV, and can be prepared with using low temperature technology such as DC magnetron sputtering, CVD^[10,11]. So the ZnO is a promising candidate to be used as HRT layer in CdTe thin film solar cells.

UPS and XPS-deep profiling were applied to investigate the interface characterization of ITO/ZnO and ZnO/CdS films, and energy band diagrams of the ITO/ZnO and ZnO/CdS were illustrated. Furthermore, numerical simulations of different ZnO properties have been done, employing the widely used AMPS-1D (analysis of microelectronic and photonic structures)^[10].

2. Experiment

ZnO films were deposited on ITO-coated quartz glass by DC magnetron sputtering (JS500-6/D, Nanguang Instrument). The target was metallic Zn (99.999%). The substrate was held at 300 °C and the deposition apparatus is 81 W. The working pressure is 2.4 Pa of high purity argon (99.999%) mixed with 30% oxygen. The sputtering procedure took 107 min and the ZnO films were about 150 nm. The CdS layers were deposited by chemical bath deposition (CBD), and were about 150 nm thick. The CdTe layers were deposited by closed-space sublimation (CSS) technology, and the thickness was about 6 μm. The back contact CdZn:Cu films were deposited using the co-vacuum evaporation method and were about 80 nm.

The structural property of the as-deposited ZnO films were analyzed by X-ray diffraction (DX-2500, Dandong Fangyuan Instrument LLC) using CuKα radiation ($\lambda = 0.15405$ nm). The sheet resistance was measured with a Digital Four Probe Tester (SZT-2, Suzhou Tongchuan Electronics). Measurement of the film thickness was done with a stylus profiler (XP-2, Ambios Technology Inc.). The optical transmission was obtained using a UV/Vis spectrometer (Perkin Elmer Inc., Lambda-950). The XPS and UPS measurements were carried out in an AXIS-ultra-DLD photoelectron spectrometer. The spectra were obtained using constant analyzer energy with He ($h\nu = 21.2$ eV) in a UHV system (the base pressure was below $5.0 \times$

* Project supported by the State Key Development Program for Basic Research of China (No. 2011CBA00708).

[†] Corresponding author. Email: zhangjingquan@263.net

Received 21 February 2012, revised manuscript received 16 April 2012

© 2012 Chinese Institute of Electronics

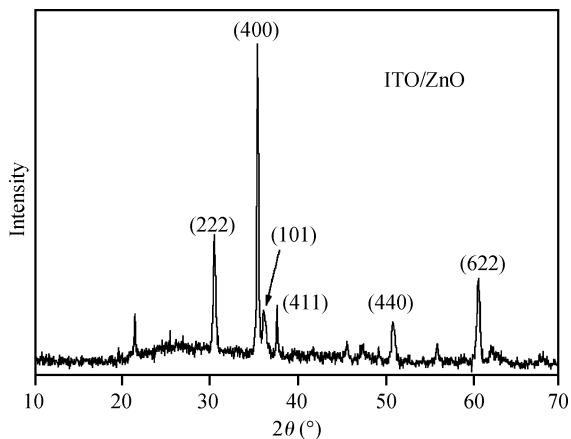


Fig. 1. X-ray diffraction of ITO/ZnO thin films.

10^{-9} Torr). For excitation, monochromatized $AlK\alpha$ radiation (1486.6 eV) was used. The Fermi level position was aligned to a binding energy $E_{bin} = 0$ eV using Ag samples.

The AMPS-1D was based on Poisson's equation, the hole and electron continuity equations in one dimension^[11]. It was used to estimate the band diagram and carrier transport. The effects of ZnO thickness, carrier density and electron mobility on CdTe solar cells were simulated.

3. Results and discussion

Figure 1 shows the XRD spectrum of as-deposited ITO/ZnO films. The main peaks come from the ITO film. It presents only one peak at 36.10° corresponding to the (101) peak diffraction of the hexagonal wurtzite phase. This indicates that the deposition of ZnO films onto the ITO films has different growth mechanisms compared to growth on glass.

Optical transmittance spectra (Fig. 2) of the ZnO films exhibit very high transmittance (85.27%) in the 400–1200 nm region. The optical band gap E_g can be calculated as 3.27 eV from the Tauc plot, which is very close to the theoretical value of 3.37 eV. The sheet resistance and calculated resistivity were $10^8 \Omega/\square$ and $1.5 \times 10^3 (\Omega \cdot \text{cm})^{-1}$ respectively, within one order of magnitude of the CdS layer. It is beneficial to avoid the pinhole effect of CdS films and improve the touching between the CdTe layer and the front contact^[12].

3.1. ITO/ZnO system

Before analysis with XPS/UPS, all of the samples were cleaned by sputtering with He^+ ions for 1 min in HUV to eliminate surface factors. The layers were profiled using XPS and UPS by taking spectra after each profiling time until it revealed the ITO films.

Figure 3 illustrates the characterization of ITO/ZnO at different profiling times. It shows the valence band maximum (E_{VBM}) increases from 3.11 to 3.21 eV at the interface of the ITO/ZnO films. The “valence band offset” at low binding energy corresponds to the $E_F - E_{VBM}$ and provides a direct measure of the Fermi level at the sample surface. At the other end of the schematic UPS spectrum the secondary electron onset, referenced to the 21.22 eV Helium source energy, provides a direct measure of the specimen's work function ($E_{vac} - E_F$).

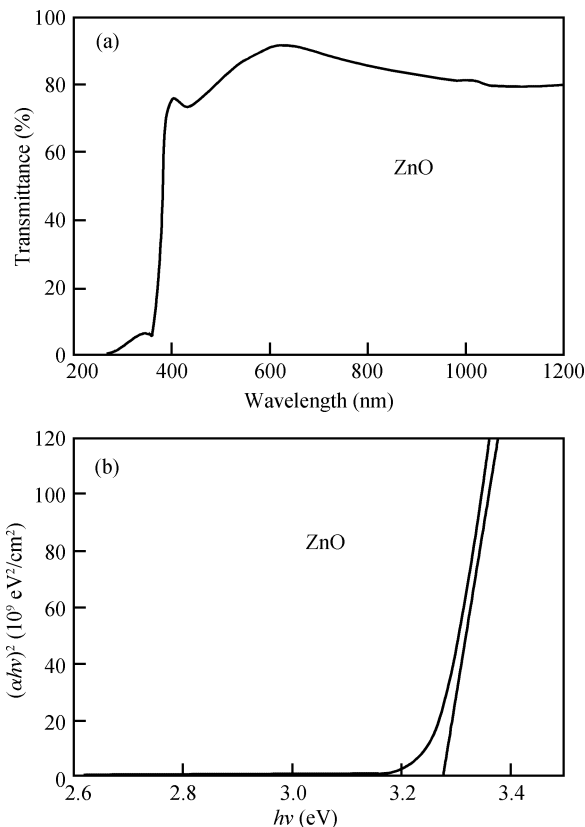


Fig. 2. (a) Transmission spectra and (b) plot of $(\alpha hv)^2$ versus hv of the ZnO thin films.

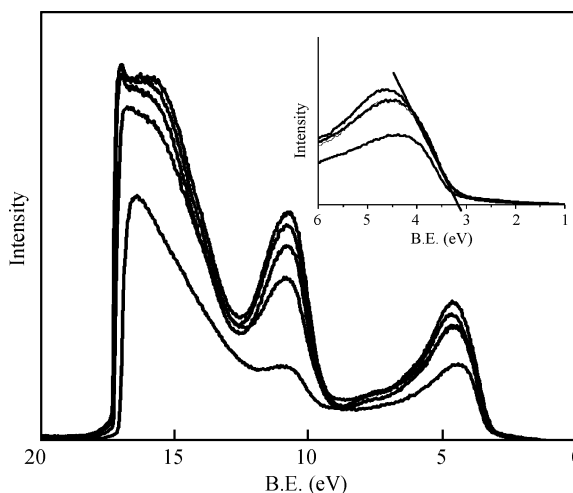


Fig. 3. UPS spectra of ITO/ZnO thin films.

The work functions were determined from the low-kinetic energy cut-off in the UPS spectra (the intersection of the linear extrapolation with the baseline).

Figure 4 shows the evolution of the In3d peak and Zn2p peak of the ITO/ZnO films. A significant increase in the intensity of In3d was observed for the sample. The work function and interface dipole can be obtained by the XPS/UPS spectra: $\delta = 0.05$ eV. And the valence band offset ΔE_V and conduction band offset ΔE_C were calculated as 0.05 eV and 0.4 eV, respectively.

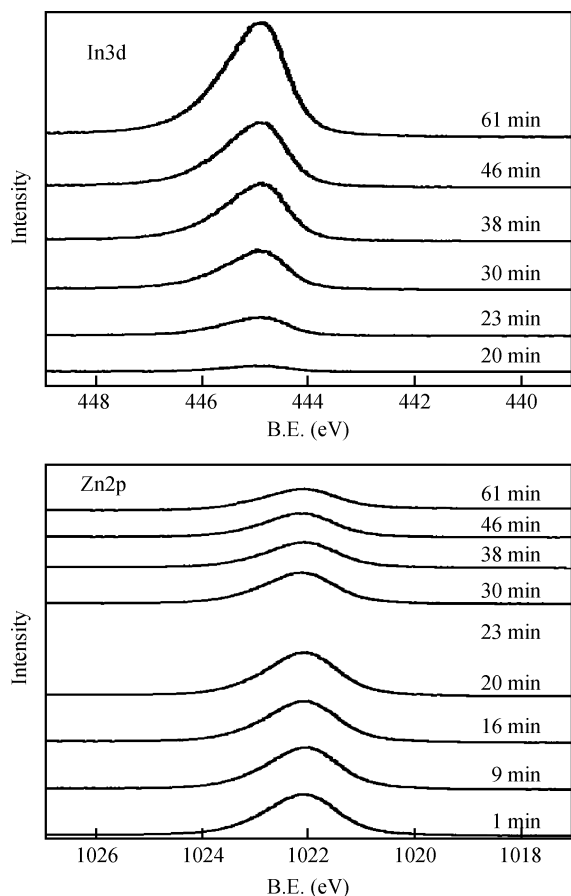


Fig. 4. XPS spectrum in the In3d and Zn2p regions for n-ITO/n-ZnO isotype heterojunction under various profiling times.

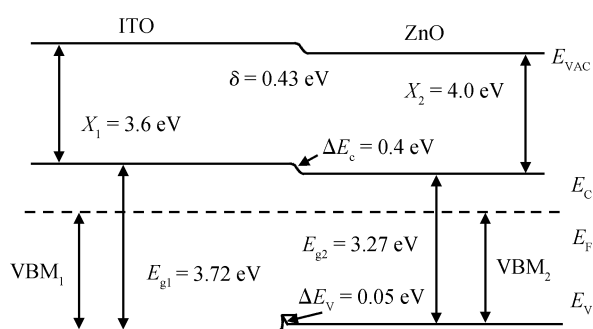


Fig. 5. Energy band diagram of the ITO/ZnO isotype heterojunction.

The final band alignment at the interface ITO/ZnO heterojunction is presented in Fig. 5. The difference between the vacuum energy (E_{vac}) and the conduction band energy is the electron affinity. The results show that the conduction band bends downward in the ITO layer at the interface while the ZnO films bends upward. The barrier energy is about 0.4 eV, which is lower than that of the ITO/CdS heterojunction potential energy barrier (0.9 eV). So the introducing of the ZnO film as a HRT layer is beneficial for the transfer of electrons from the CdS films to the ITO films.

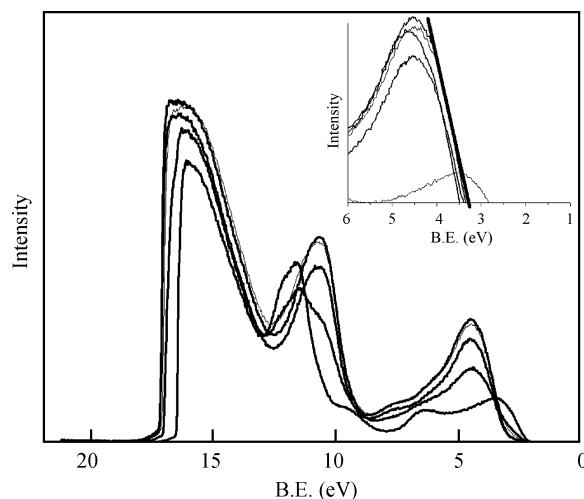


Fig. 6. UPS spectra of ZnO/CdS thin films.

3.2. ZnO/CdS system

Samples were also cleaned by sputtering with He^+ ions for 1 min. The XPS and UPS spectra were obtained for each profiling time. Figure 6 shows the characterization of ZnO/CdS at different profiling times. It shows that the E_{VBM} decreases from 3.18 to 2.0 eV at the interface of the ZnO/CdS films during the profiling. The difference of the E_{VBM} value of ZnO films is attributed to the different ambience in the ITO/ZnO and in the ZnO/CdS systems.

Figure 7 shows the evolution of the Cd3d peak and Zn2p peak of the ZnO/CdS films. A significant increase of the intensity of Zn2p was observed for the sample. The interface dipole can be obtained: $\delta = 0.23$ eV. And ΔE_v and ΔE_c were calculated as 0.45 eV and 0.5 eV, respectively.

The band alignment at the interface ZnO/CdS heterojunction is presented in Fig. 8. The energy barrier is about 0.5 eV, which would not obstruct the transfer of electrons from the CdS to ZnO films.

3.3. Application to the CdTe solar cells

We fabricated the CdTe solar cells by depositing ZnO films on ITO coated glass. The CdS and CdTe films were deposited by CBD and CSS, respectively. Figure 9 shows the current-voltage curve of the CdTe solar cell with or without ZnO HRT films. The sample with the ZnO films has the efficiency of 12.77% ($V_{oc} = 857$ mV, $J_{sc} = 21$ mA/cm², FF = 70.7%, area = 0.5 cm²) while the sample without the ZnO films has a much lower efficiency of 8.9% ($V_{oc} = 783$ mV, $J_{sc} = 24$ mA/cm², FF = 70.7%, area = 0.5 cm²). The cell with the HRT films also showed a low series resistance and a high fill factor, which was partly attributed to good interface properties between the n-ZnO and CdS layers. Figure 10 shows the quantum efficiency curve of samples with or without the ZnO films. The QE of cells with the ZnO films (> 90%) are higher than the QE without the ZnO films (79%).

3.4. Influence of thickness, mobility and carrier density of ZnO in CdTe solar cells

In this reference, the influence of ZnO thickness, mobility

Table 1. Parameters in AMPS-1D simulation.

Parameter	ITO	ZnO	CdS	CdTe
E_g (eV)	3.72	3.27	2.42	1.46
EPS	9.4	9	9	9.4
Electron mobility ($\text{cm}^2/(\text{V}\cdot\text{s})$)	30	60–100	340	500
Hole mobility ($\text{cm}^2/(\text{V}\cdot\text{s})$)	5	25	50	60
Carrier density (cm^{-3})	4.3×10^{20}	10^{16} – 10^{19}	10^{17}	2×10^{15}
Density of state, CB (cm^{-3})	4×10^{19}	1.8×10^{19}	1.8×10^{19}	7.5×10^{17}
Density of state, VB (cm^{-3})	10^{18}	2.4×10^{18}	2.4×10^{18}	1.8×10^{18}
Electron affinity	3.6	4	4.5	4.28
Thickness (μm)	0.4	0–0.8	0.15	6

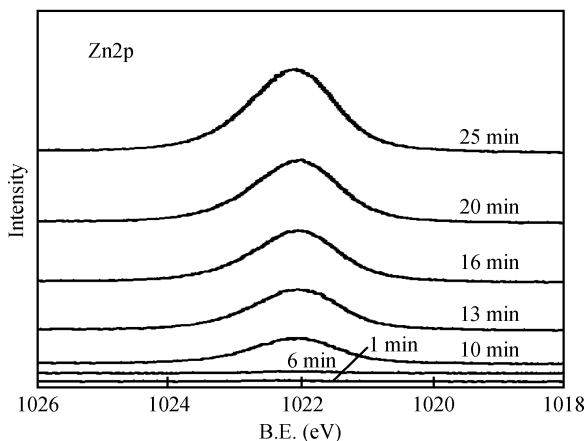
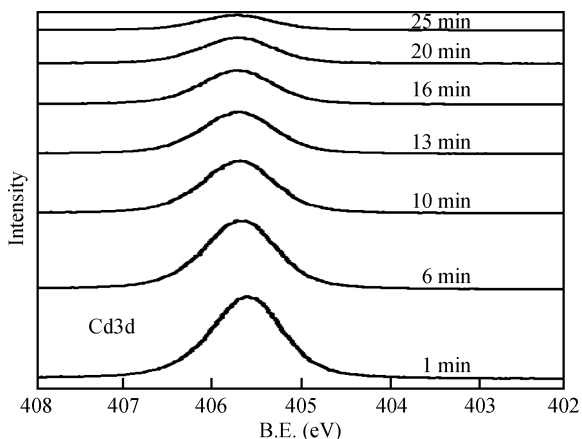


Fig. 7. XPS spectrum in the Cd3d and S2p reigns for n-ZnO/n-CdS isotype heterojunction under various profiling times.

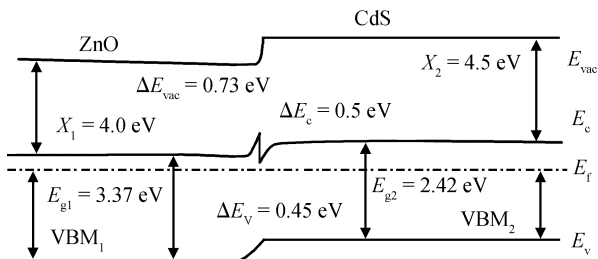


Fig. 8. Band diagram of the n-ZnO/n-CdS isotype heterojunction.

and carrier density on CdTe solar cells were studied further by AMPS-1D simulation. The parameters used in the simulation are shown in Table 1. The electron affinity energies and mobil-

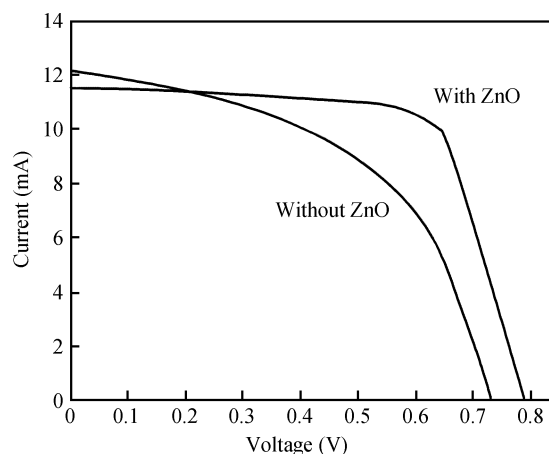


Fig. 9. I - V curve of the CdTe solar cell with or without ZnO films.

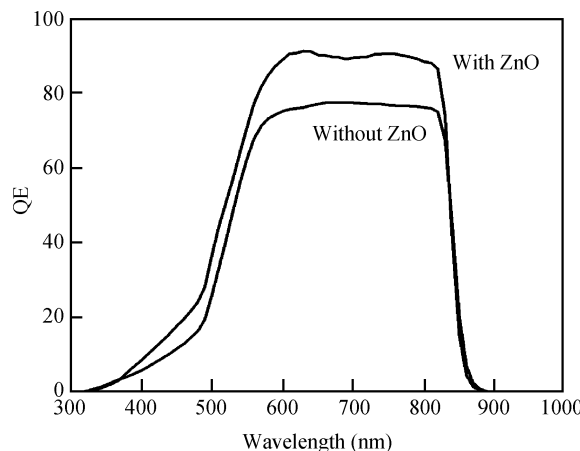


Fig. 10. QE curve of the CdTe solar cell with or without ZnO films.

ity were obtained from Refs. [15, 16]. To simplify this calculation, we assumed that the working temperature is 300 K, there is no light trapping and the surface recombination velocity is 10^7 cm/s [17].

The first result obtained from the calculation is the effect of ZnO thickness on the CdTe solar cell characteristics. The ZnO thickness was changed from 150 to 800 nm. As shown in Fig. 11, the insertion of the ZnO film significantly increases the energy conversion efficiency E_{ff} , owing to the increase in short-circuit current density (J_{sc}) and open-circuit voltage (V_{oc}), which is in agreement with the experiment results. All

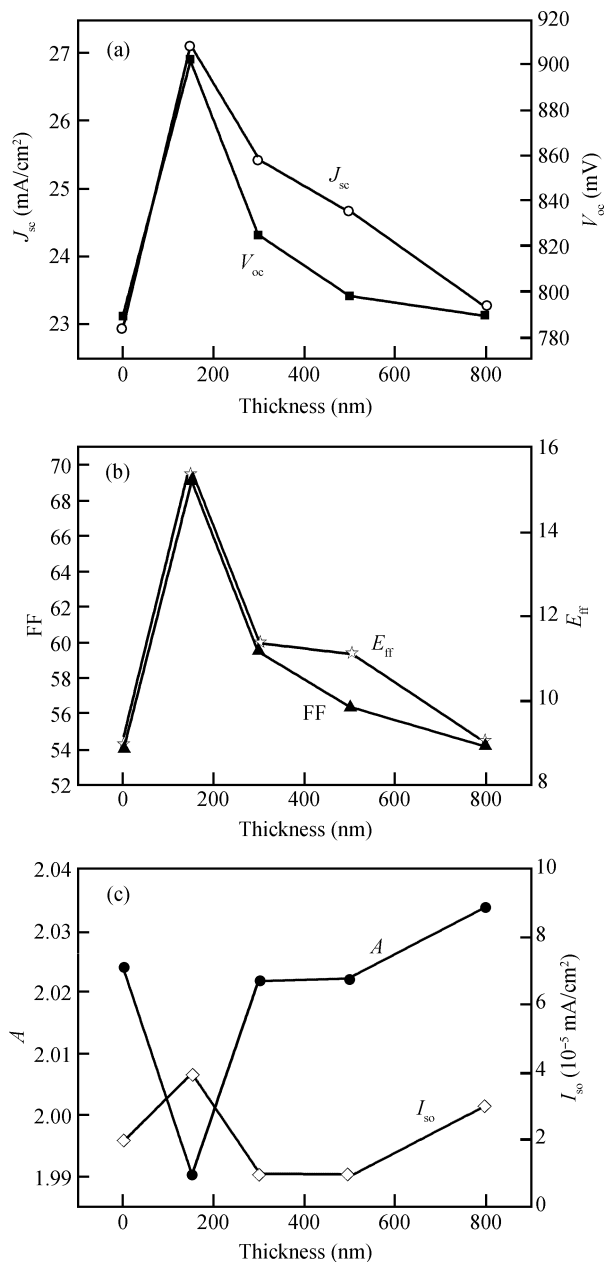


Fig. 11. Effect of the ZnO film thickness on the performance of the CdTe solar cell.

the characteristics increased drastically for film thicknesses below 150 nm, while they decreased at thickness of 150–800 nm. This is because with the increase in the thickness of the film, the built-in electric field intensity distribution is significantly affected. The photogenerated charge carriers will not be effectively collected, so all the characteristics decreased with the increase in film thickness. The maximum value of E_{ff} is achieved when the thickness is about 150 nm. Also the ideal diode factor (A) and reverse saturation current density (I_0) were obtained. The minimum A and maximum I_0 were also obtained at 150 nm.

Figure 12 shows the variation of E_{ff} in the CdTe solar cell with the change of carrier density (10^{16} to 10^{19} cm⁻³) and electron mobility (40 to 100 cm²/(V·s)) of the ZnO film, where the thickness is fixed at 150 nm. The E_{ff} increased significantly

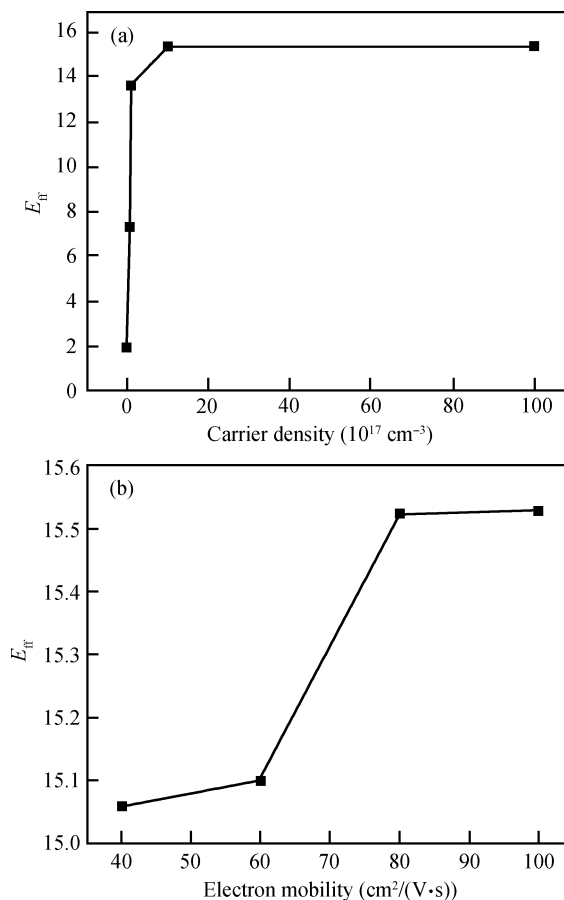


Fig. 12. Effect of (a) carrier density and (b) electron mobility of the ZnO film on E_{ff} .

as the carrier density increased and reached its highest value. The E_{ff} increased little with the increase of the electron mobility.

4. Conclusions

The ZnO films were successfully deposited on the ITO films by the DC magnetron sputtering method. The transmittance in the visible region (85.27%) and sheet resistance ($10^8 \Omega/\square$) are obtained. The characterization at the interface of the ITO/ZnO and ZnO/CdS were studied by UPS and XPS deep profiling. The energy band diagrams were depicted, and the energy barrier at the interface of ITO/ZnO and ZnO/CdS films were almost 0.4 eV and 0.5 eV, they are much lower than that in ITO/CdS. So the insertion of the ZnO films most likely results in a strongly reduced minority carrier recombination at the interface.

CdTe thin film solar cells with or without ZnO films were prepared. The energy conversion efficiency and quantum efficiency were found to be 12.77% (8.9%) and > 90% (79%) with or (without) the ZnO films. Furthermore, we have also simulated and analyzed the effect of the ZnO films on the CdTe cells using AMPS-1D. The results show that inserting a ZnO film in a CdTe solar cell significantly improves its efficiency, which reached its highest value when the thickness of the ZnO film was 150 nm. Carrier density and electron mobility have different effects on E_{ff} in CdTe solar cells.

References

- [1] Wu Xuanzhi. High-efficiency polycrystalline CdTe thin-film solar cells. *Solar Energy*, 2004, 77(6): 803
- [2] Romeo N, Bosio A, Canevari V, et al. Recent progress on CdTe/CdS thin film solar cells. *Solar Energy*, 2004, 77(6): 795
- [3] Ferekides C S, Marinsky D, Viswanathan V, et al. High efficiency CSS CdTe solar cells. *Thin Solid Films*, 2000, 361/362: 520
- [4] Morales-Acevedo A. Thin film CdS/CdTe solar cells: research perspectives. *Solar Energy*, 2006, 80(6): 675
- [5] Ferekides C S, Mamazza R, Balasubramanian U, et al. Transparent conductors and buffer layers for CdTe solar cells. *Thin Solid Films*, 2005, 480: 224
- [6] Klein A, Körber C, Wachau A, et al. Transparent conducting oxides for photovoltaics: manipulation of Fermi level, work function and energy band alignment. *Materials*, 2010, 3(11): 4892
- [7] Mahabaduge H, Wieland K, Compaan A. Influence of a high resistivity transparent (HRT) layer on the performance of CdTe solar cells. Spring Meeting of the Ohio Section of the APS, 2010, 55(4): B2.004
- [8] Alamri S N, Brinkman A W. The effect of the transparent conductive oxide on the performance of thin film CdS/CdTe solar cells. *J Phys D: Appl Phys*, 2000, 33: L1
- [9] Fuchs H, Schimper J, Klein A, et al. Photoemission studies on undoped SnO₂ buffer layers for CdTe thin film solar cells. *Energy Procedia*, 2011, 10: 149
- [10] Klingshirn C. The luminescence of ZnO under high one- and two-quantum excitation. *Phys Status Solidi B*, 1975, 71: 547
- [11] Özgür Ü, Alivov Y I, Liu C, et al. A comprehensive review of ZnO materials and devices. *J Appl Phys*, 2005, 9(4): 103
- [12] Krajangsang T, Afdi Yunaz I, Miyajima S, et al. Effect of p- μ -Si_{1-x}O_x:H layer on performance of hetero-junction microcrystalline silicon solar cells. *Current Applied Physics*. 2010, 10(3): s357
- [13] Bouloufa A, Djessas K, Zegadi A. Numerical simulation of CuIn_xGa_{1-x}Se₂ solar cells by AMPS-1D. *Thin Solid Films*, 2007, 515(15): 6285
- [14] Chopra K L, Paulson P D, Dutta V. Thin-film solar cells: an overview. *Prog Photovolt: Res Appl*, 2004, 12: 69
- [15] Matin M A, Aliyu M M, Quadery A H, et al. Prospects of novel front and back contacts for high efficiency cadmium telluride thin film solar cells from numerical analysis. *Solar Energy Materials and Solar Cells*, 2010, 94(9): 1496
- [16] Fonash S J. *Solar cell device physics*. New York: Academic-Press, 1981
- [17] Lin Aiguo, Ding Jingning, Yuan Ningyi, et al. Analysis of the p⁺/p window layer of thin film solar cells by simulation. *Journal of Semiconductors*, 2012, 33(2): 023002